Fragment-Based Approach for Estimating Thermophysical Properties of Fats and Vegetable Oils for Modeling Biodiesel Production Processes

Li Zong

AspenTech Limited, Pudong, Shanghai 201203, People's Republic of China

Sundaram Ramanathan and Chau-Chyun Chen*

Aspen Technology, Inc., Burlington, Massachusetts 01803

A fragment-based methodology for estimating the thermophysical properties of triglycerides is presented. In contrast to the commonly practiced functional group estimation approach, the proposed methodology adopts a chemical constituent fragment-based approach to estimate the triglyceride pure component properties from fragment composition and parameters of the fragments. The fragment-specific parameters are obtained from regressing against very limited experimental data for triglycerides available in the literature. The methodology further explores the relationships between carbon atom numbers of fatty acid constituent fragments and the values of these fragment-specific parameters. Additionally, the effect of the double bonds on the values of these fragment-specific parameters is investigated. Based on this methodology, we develop the first-ever pure component thermophysical property databank of triglycerides. We show satisfactory predictions on the properties of triglycerides, fats, and oils. We further show the superiority of this methodology over the traditional functional group approach. The methodology, the derived databank, together with the currently available databanks for fatty acids and corresponding esters, enable efficient and reliable thermophysical property calculations in support of process modeling, simulation, design, and optimization of biodiesel production processes.

Introduction

Biodiesel is a renewable alternative diesel fuel consisting of long-chain alkyl (methyl or ethyl) esters, made by transesterification of vegetable oils such as those from corn, olive, palm, and sunflower; animal fats such as tallow, lard, and butter; and commercial products such as margarines. Over the past decade, interest has grown tremendously in the use of fats and vegetable oils as a feedstock for manufacturing biodiesel, and many commercial biodiesel plants have been built. However, the economic advantage of using vegetable oils as a biodiesel feedstock can vary significantly, depending on factors such as fluctuating cost of crude oil, limited supply of vegetable oils, and competing demands in food applications.

Many research activities have focused on the development of new nonfood vegetable oil sources as a sustainable feedstock for biodiesel manufacturing. For example, certain species of algae that contain high amounts of oil and have high growth rates are considered to be a promising potential feedstock for next-generation biofuel. New feedstock, combined with new process technologies and optimized production plants, can help alleviate some of the cost pressures and accelerate the trend toward renewable alternatives.

Process modeling and simulation is an established best practice for rapid process development and optimization in the chemical and petrochemical industry. Such technology is also contributing to the development and optimization of biodiesel process technologies and production plants. However, one of the challenges limiting the use of process modeling and simulation with biodiesel production processes is the lack of proven models and databanks for estimating thermophysical properties of vegetable oils, blends, and, most importantly, the

individual triglyceride components that comprise the oils. Triglycerides, which are also known as triacylglycerols (or TAGs), are the major components of almost all of the commercially important fats and oils of animals and plant origin.[1,2] Accurate estimation of the thermophysical properties of triglycerides is an essential prerequisite to the effective use of process modeling and simulation technology for design, optimization, and control of biodiesel manufacturing processes. In this paper, we compile and examine available experimental data for triglycerides. We present a novel constituent fragment-based method for systematic correlation and accurate estimation of thermophysical properties of individual triglyceride components. We further validate the estimation methodology with satisfactory predictions for the properties of fats and oils.

Characterization of Fats and Oils. The main constituents of vegetable oils and animal fats are triglycerides. Triglycerides can be formed from the condensation reaction of glycerol and fatty acids,[3] as illustrated in Figure 1.

The chemical formula of triglycerides is $RCOO-CH_2CH(-OOCR')CH_2-OOCR''$, where R, R', and R'' are long alkyl or alkenyl chains. The three fatty acids—RCOOH, R'COOH, and R''COOH—can be all different, all the same, or only two the same.[1] Triglycerides with three identical fatty acids are
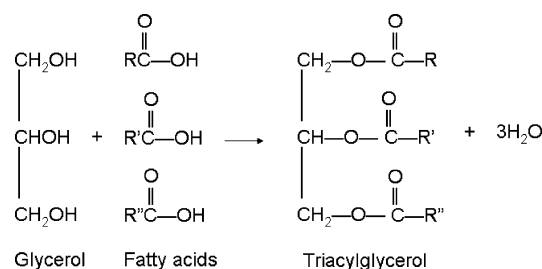

Figure 1. Condensation reaction for the formation of triglycerides.

* To whom correspondence should be addressed. Tel.: 781-221-6420. Fax: 781-221-6410. E-mail: chauchyun.chen@aspentech.com.

Table 1. Names and Symbols for Common Fatty Acids

trivial name	symbol	numerical symbol
butyric acid	Bu	C4:0
caproic acid	Co	C6:0
caprylic acid	Cy	C8:0
capric acid	C	C10:0
lauric acid	L	C12:0
myristic acid	M	C14:0
palmitic acid	P	C16:0
palmitoleic acid	Po	C16:1
stearic acid	S	C18:0
oleic acid	O	C18:1
linoleic acid	Li	C18:2
α-linolenic acid	Ln	C18:3
arachidic acid	A	C20:0
behenic acid	B	C22:0
erucic acid	E	C22:1

Table 2. Triglyceride Profile for Crude Cottonseed Oil[a]

triglyceride	composition (wt %)	triglyceride	composition (wt %)
LOP	0.09	POLi	14.3
PPoP	0.62	SOLi	1.31
POP	3.67	OLiA	0.09
POS	0.54	LLiLi	0.23
POA	0.07	MLiLi	1.11
LLiP	0.26	PLiLi	26.58
MLiP	1.16	SLiLi	4.75
PLiP	13.74	LiLiA	0.17
PLiS	3.91	PoLiLi	1.3
PLiA	0.39	OLiLi	10.43
LOLi	0.19	LiLiLi	12.88
PPoLi	1.93	LiLiLn	0.28

[a] Data taken from ref 5. The sum of all compositions is 100%.

usually called simple triglycerides. Triglycerides that contain more than one type of fatty acid chain are called mixed triglycerides. Chain lengths of the fatty acids in natural triglycerides are variable; however, 16, 18, and 20 carbons are the most common.

Triglyceride structure is classified by the fatty acids present and by the point of attachment of each fatty acid to the glycerin. Triglycerides are designated by an acronym representing the three individual fatty acids and their order in the glycerol portion of the molecule. For example, trimyristin is composed of three myristic acids and tripalmitin is made from three palmitic acids. Thus, trimyristin can be denoted by MMM and tripalmitin by PPP. A mixed triglyceride made from two palmitic acids in the outer positions and one myristic acid in the middle position of the glycerol portion can be denominated as PMP.[2−7] Table 1 lists symbols for various fatty acids used throughout the paper, using this naming convention.

Triglyceride molecules are also denoted by a convenient shorthand designation showing the number of carbon atoms and the number of double bonds of the constituent fatty acids.[8] (See the numerical symbols for the fatty acids in Table 1.) Thus, small squares (Figure 2) are used to represent the fatty acid components of triglycerides.[9] Each square symbolizes the fatty acid components of a representative triglyceride molecule. Red is used for saturated fatty acids, green for monounsaturated fatty acids, and blue for polyunsaturated fatty acids.

Most natural fats and oils are complex mixtures of many different triglycerides. The exact triglyceride composition of a fat or oil further varies with the sources and growth conditions. Different notations are used to characterize the triglyceride composition of a fat or oil. For example, Table 2 illustrates the average triglyceride composition in weight percentages of crude cottonseed oil estimated by Ceriani and Meirelles,[5] following the composition measurement procedure of Antoniosi Filho et al.[6]

Another approach to represent the triglyceride composition of a fat or oil is shown in Figure 3, using lard as an example.[9] The percentages (by weight) of total fatty acids in lard are ~2% myristic acid (C14:0), ~26% palmitic acid (C16:0), ~14% stearic acid (C18:0), ~44% oleic acid (C18:1), ~10% linoleic acid (C18:2), and other constituents. These fatty acid fragments would be distributed randomly among the 33 representative triglyceride molecules in Figure 3.

Figure 2. Triglyceride characterization for SSS, OOP, and LiOS.

Many triglyceride components must be considered when calculating the thermophysical properties of a given oil or fat. Unfortunately, except for a few simple triglycerides, experimental thermophysical property data are rarely available for triglycerides. A validated methodology is required to estimate thermophysical properties of triglycerides—and, therefore, oils and fats—accurately for process modeling and simulation calculations.

Estimating Thermophysical Properties in Support of Process Modeling and Simulation. Pure-component properties that are essential for process modeling and simulation include vapor pressure, enthalpy of vaporization, liquid heat capacity, enthalpy of formation, liquid density, and liquid viscosity. Such pure-component properties must become available for all of the triglycerides before complete characterization of biodiesel feedstock can be made in process modeling and simulation and meaningful phase equilibrium and process calculations can be performed in designing and optimizing biodiesel production processes. An inability to characterize biodiesel feedstock, in terms of the full spectrum of triglyceride molecules, diminishes the fidelity of the process models and lessens the quality of the engineering decisions made with the process models.

In this work, we show the development of a databank for triglycerides formed with common saturated and unsaturated fatty acid fragments, i.e., C12:0, C14:0, C16:0, C18:0, C18:1, C18:2, C18:3 and C20:0. Table 3 shows the name and chemical structure of these fragments. Note that the distribution of the fatty acids is reported to be nonrandom, because the unsaturated fatty acids are positioned predominately in the middle/beta position (sn-2) of the glycerol portion of the molecule and the saturated fatty acids are positioned predominately in the alpha or outer positions (sn-1 and sn-3).[10] Here, the prefix "sn" represents stereospecific numbering. Accordingly, mixed triglycerides that contain one unsaturated fatty acid have only two forms instead of six forms. For example, the triglycerides that are composed of the three different fatty acids P [C16:0], S [C18:0], and O [C18:1] should be POS and SOP. The triglycerides PSO, SPO, OSP, and OPS are regarded as nonexistent, and thus are not included in the databank.

For completeness, pure-component critical properties such as critical temperature (T_c) and critical pressure (P_c) are also included in the databank. These critical properties are required for use with cubic equations-of-state (EOSs), which are often used to compute vapor-phase fugacity coefficients in process simulators. However, triglyceride molecules, being relatively large molecules, have very low vapor pressure and the biodiesel production processes normally operate under vacuum conditions. Therefore, the choice of cubic EOS and the corresponding critical properties have little impact on the simulation results for biodiesel production processes. Furthermore, accurate de-

Figure 3. Triglyceride profile for lard.

Table 3. Fragments Included in the Triglyceride Databank

fragment	carbon atom	symbol	chemical structure
glycerol		Gly-frag	$-OCH_2CH(O-)CH_2O-$
lauric	C12:0	L-frag	$CH_3(CH_2)_{10}CO-$
myristic	C14:0	M-frag	$CH_3(CH_2)_{12}CO-$
palmitic	C16:0	P-frag	$CH_3(CH_2)_{14}CO-$
stearic	C18:0	S-frag	$CH_3(CH_2)_{16}CO-$
oleic	C18:1	O-frag	$CH_3(CH_2)_7CH=CH(CH_2)_7CO-$
linoleic	C18:2	Li-frag	$CH_3(CH_2)_4CH=CHCH_2CH=CH(CH_2)_7CO-$
linolenic	C18:3	Ln-frag	$CH_3CH_2CH=CHCH_2CH=CHCH_2CH=CH(CH_2)_7CO-$
arachidic	C20:0	A-frag	$CH_3(CH_2)_{18}CO-$

termination of critical properties for triglyceride molecules would not be possible, because the molecules would have decomposed before these critical properties could be determined. We use standard functional group contribution methods in Aspen Plus for rough estimation of the T_c and P_c values for the triglyceride molecules.

Given the pure-component properties for triglycerides, one could then apply proper activity coefficient models to perform various phase equilibrium calculations such as vapor−liquid equilibrium, liquid−liquid equilibrium, or vapor−liquid−liquid equilibrium. However, because of the lack of available experimental phase equilibrium data for binary systems involving triglycerides, one could not rely on commonly practiced engineering activity coefficient models such as NRTL or UNIQUAC. Use of these correlative engineering models requires determination of binary interaction parameters for each and every binary system from phase equilibrium data for each binary system. Until such phase equilibrium data become available, the predictive UNIFAC group-contribution activity coefficient model remains the only choice for phase equilibrium calculations involving triglycerides. Fortunately UNIFAC has been shown to provide adequate representation for the liquid-phase nonideality for systems involving linear organic molecules such as fatty acids, alcohols, and triglycerides.

Functional Group Approach versus Constituent Fragment Approach. There are a few published works on the estimation of pure-component thermophysical properties for triglycerides, and they are mainly based on the traditional functional group approach. For example, Ceriani and Meirelles[5] reported a group contribution method for the estimation of the vapor pressure of fatty compounds. They split the fatty compounds into eight functional groups: CH_3, CH_2, COOH, CH=cis, CH=trans, OH, COO, and $CH_2-CH-CH_2$. The same authors later extended this functional group approach to predict the viscosity of triglycerides.[11] Separately, there exists a group-contribution method that was developed to predict melting points and enthalpies of fusion of saturated triglycerides.[12]

In fact, the Aspen Plus process simulator offers several established functional group models and built-in parameters to estimate pure-component properties for any compounds, including triglycerides. However, although the functional group approach is well-established and one could easily identify sets of functional groups and parameters to estimate and perhaps match certain data for triglycerides, we have found that the functional group approach is too simplistic to provide sufficient fidelity for thermophysical properties of various triglycerides. In a later section, we show that the functional group approach does not provide sufficient accuracy for the estimation of thermophysical properties of triglycerides.

Instead, we propose a chemical constituent fragment-based approach to estimate thermophysical properties for triglycerides and their mixtures. The proposed fragment approach offers perhaps the optimal level of estimation accuracy and parameter abstraction. With the fragment-based approach, the triglyceride components are considered to be compounds that are comprised of a backbone glycerol fragment with three fatty acid fragments attached, and the thermophysical properties of a triglyceride component are calculated from the composition of the constituent fragments and sets of fragment-specific parameters. Figure 4 shows a structural characterization of a glycerol fragment and three fatty acid fragments for an example triglyceride molecule. The fragment-based approach allows accurate estimation of the pure-component properties of mixed triglycerides from available experimental data for simple triglycerides. It further allows us to explore the relationships between carbon atom numbers of fatty acid constituent fragments and values of their fragment-specific parameters. Additionally, the effect of double bonds on the values of these fragment-specific parameters can be systematically investigated. The only effect that is not addressed by the fragment-based approach is the stereospecific effect, because the proposed approach assumes that the contribution of each fatty acid fragment to the properties of triglyceride compounds is independent of position of the fatty acid fragment on the glycerol backbone fragment. On the other hand, to our knowledge, no experimental data are available in the literature for us to explore such stereospecific effect with triglycerides.

Determination of Fragment-Specific Parameters. The fragment-specific parameters for calculating thermophysical properties of triglycerides must be regressed from the very limited experimental data available in the open literature. The following sections discuss how we identify fragment-specific parameters for selected pure-component properties: vapor pressure, enthalpy of vaporization, liquid heat capacity, enthalpy of formation, liquid molar volume, and liquid viscosity.
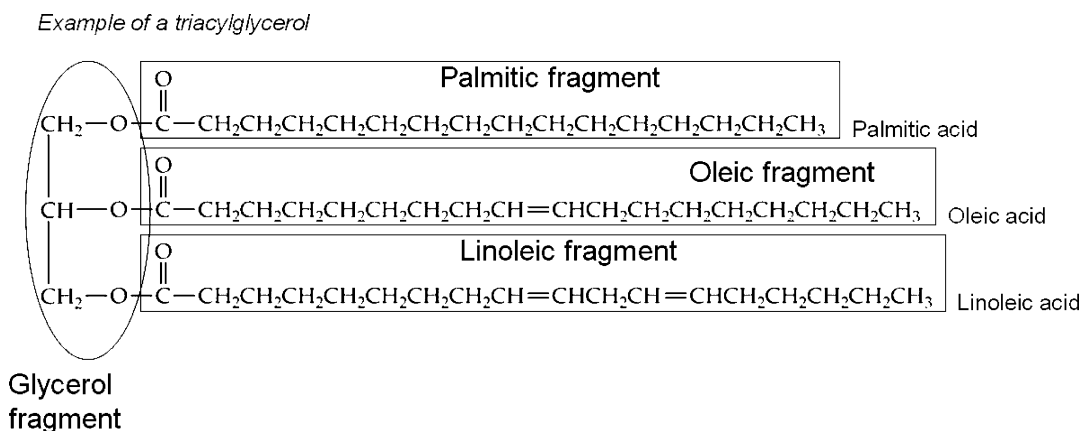
Example of a triacylglycerol

Figure 4. Fragment characterization for a triglyceride.

Table 4. Calculated Physical Constants from Vapor Pressures of Triglycerides

material	carbons	A	B	ΔH_θ^{vap} (J/kmol)	ΔG_θ^{vap} (J/kmol)
tributyrin	4:4:4	9.495	4250	8.137×10^7	2.717×10^7
tricaproin	6:6:6	9.945	4950	9.477×10^7	3.800×10^7
tricaprylin	8:8:8	11.245	6060	1.160×10^8	5.183×10^7
tricaprin	10:10:10	11.205	6510	1.246×10^8	6.067×10^7
trilaurin	12:12:12	11.705	7190	1.377×10^8	7.084×10^7
trimyristin	14:14:14	11.905	7720	1.478×10^8	7.984×10^7
tripalmitin	16:16:16	12.525	8400	1.608×10^8	8.932×10^7
tristearin	18:18:18	12.725	8750	1.675×10^8	9.488×10^7
1-capryl-2-lauryl-3-myristin	10:12:14	11.025	6880	1.317×10^8	6.879×10^7
1-lauryl-2-myristyl-3-palmitin	12:14:16	11.925	7720	1.478×10^8	7.973×10^7
1-myristyl-2-palmityl-3-stearin	14:16:18	12.305	8250	1.579×10^8	8.771×10^7
1-myristyl-2-capryl-3-stearin	14:10:18	12.005	7750	1.484×10^8	7.985×10^7
1-myristyl-2-lauryl-3-stearin	14:12:18	11.965	7860	1.505×10^8	8.218×10^7
1-palmityl-2-capryl-3-stearin	16:10:18	12.425	8090	1.549×10^8	8.396×10^7
1-palmityl-2-lauryl-3-stearin	16:12:18	12.675	8360	1.601×10^8	8.770×10^7

Vapor Pressure and Enthalpy of Vaporization. We estimate vapor pressures of triglyceride components from the following Clausius−Clapeyron equation:

$$\log P(T) = A - \frac{B}{T} = \frac{-\Delta G_\theta^{vap}}{R\theta \ln 10} + \frac{\Delta H_\theta^{vap}}{R \ln 10}\left(\frac{1}{\theta} - \frac{1}{T}\right) \quad (1)$$

where A and B are vapor pressure temperature dependency parameters; P is the vapor pressure (in units of Pa), T the temperature (in Kelvin), R the gas constant, θ the reference temperature ($\theta = 298.15$ K), ΔH_θ^{vap} the enthalpy of vaporization at reference temperature θ, and ΔG_θ^{vap} the Gibbs free energy of vaporization at reference temperature θ.

Equation 1 relates the vapor pressure and the temperature with the enthalpy and the Gibbs free energy of vaporization.[13] Perry[14] reported the vapor pressure temperature dependency parameters for some common simple and mixed triglycerides. The relationships cover the temperature range from 323.15 K to 573.15 K. We first identify ΔH_θ^{vap} and ΔG_θ^{vap} parameters from the parameters reported by Perry for the triglycerides and eq 1. Table 4 lists these calculated ΔH_θ^{vap} and ΔG_θ^{vap} for the triglycerides investigated in Perry's paper.[14] We then apply a fragment-based additivity rule on ΔH_θ^{vap} and ΔG_θ^{vap} for triglycerides, and we identify fragment-specific enthalpy and Gibbs free energy of vaporization from triglyceride fragment compositions, as shown in eqs 2 and 3.

$$\Delta H_\theta^{vap} = \sum_A N_{frag,A}\Delta H_{\theta,A}^{vap} \quad (2)$$

$$\Delta G_\theta^{vap} = \sum_A N_{frag,A}\Delta G_{\theta,A}^{vap} \quad (3)$$

where $N_{frag,A}$ is the number of fragment A in the component, $\Delta H_{\theta,A}^{vap}$ the enthalpy of vaporization contribution of fragment A, and $\Delta G_{\theta,A}^{vap}$ the Gibbs free energy of vaporization contribution of fragment A.

The relationships between identified $\Delta H_{\theta,A}^{vap}$ and $\Delta G_{\theta,A}^{vap}$ parameters for the fragments and the carbon number of each fatty acid fragment are shown with the fitting curves eqs (a) and (b) in Table 5, along with the R^2 values of the trend line equations.

The parameters for the saturated fatty acid fragments with long chains, such as C20 and C22, can be extrapolated from the trend line equations. The calculated parameters $\Delta H_{\theta,A}^{vap}$ and $\Delta G_{\theta,A}^{vap}$, for the glycerol fragment and fatty acid fragments with carbon numbers ranging from 4 to 22, are tabulated in Table 6.

To our knowledge, experimental data for vapor pressures of unsaturated triglycerides such as trilinolein [C18:2] and trilinolenin [C18:3] are not available for us to identify the fragment-specific parameters. Until such data become available, we choose to assume that the effect of double bonds on vapor pressure of triglyceride molecules is negligible. In other words, the vapor pressure of unsaturated triglycerides is regarded as the same as that of saturated triglycerides with the same carbon numbers. Similarly, the effect of double bonds on enthalpy of vaporization and Gibbs free energy of vaporization is also assumed to be negligible.

We then use eqs 2 and 3 to estimate enthalpy of vaporization and Gibbs free energy of vaporization for any triglyceride composed of the fragments reported in Table 6. Given the enthalpy of vaporization and the Gibbs free energy of vaporization for the triglyceride, we then apply eq 1 to compute the temperature-dependent vapor pressure for the triglyceride.

Heat Capacity. The liquid heat capacities of triglycerides are calculated from the fragment composition and the fragment heat capacity parameters:

$$C_p^l = \sum_A N_{frag,A}C_{p,A}^l(T) \quad (4)$$

Table 5. Relationship between Fragment-Specific Parameters and Carbon Number of Each Fatty Acid Fragment[a]

fragment-specific parameters	trend line equation	R^2	equation number
Vapor Pressure			
$\Delta H_{\theta,A}^{vap}$ (J/kmol)	$y = 2093479.64x + 31397826.69$	0.988	(a)
$\Delta G_{\theta,A}^{vap}$ (J/kmol)	$y = 1653142.78x + 24008494.20$	0.994	(b)
Heat Capacity			
$A_{1,A}$ (J/(kmol K))	$y = 21028.920x - 2485.721$	0.995	(c)
$A_{2,A}$ (J/(kmol K^2))	$y = 31.459476x + 82.038794$	0.946	(d)
Liquid Enthalpy of Formation			
saturated (kJ/mol)	$y = -59.571x - 1358.7$	0.996	(e)
monounsaturated (kJ/mol)	$y = -76.494x - 815.18$	1.00	(f)
Solid Enthalpy of Formation			
saturated (kJ/mol)	$y = -76.467x - 1250.8$	0.995	(g)
monounsaturated (kJ/mol)	$y = -85.795x - 752.88$	0.999	(h)
Liquid Molar Volume			
$B_{1,A}$ (kmol/m^3)	$y = 65.787x^{-0.9251}$	0.999	(i)
$B_{2,A}$ (K^{-1})	$y = 3.6064 \times 10^{-6}x^2 - 7.7353 \times 10^{-5}x + 1.6438 \times 10^{-3}$	0.720	(j)
Liquid Viscosity			
$C_{1,A}$ (Pa s)	$y = -1.0172x - 45.8525$	0.898	(k)
$C_{2,A}$ (K)	$y = 81.83611x + 2153.99554$	0.943	(l)
$C_{3,A}$ (K)	$y = 0.141996x + 20.545285$	0.896	(m)

[a] Note: In the equations, y represents the fragment-specific parameters in column 1 and x represents the carbon number of each saturated fatty acid fragment. R^2 represents the R-squared values of the trend line equations.

Table 6. Calculated Vapor-Pressure Fragment Parameters $\Delta H_{\theta,A}^{vap}$ and $\Delta G_{\theta,A}^{vap}$

fragment	symbol	carbon	$\Delta H_{\theta,A}^{vap}$ (J/kmol)	$\Delta G_{\theta,A}^{vap}$ (J/kmol)
glycerol	Gly-frag		-3.476×10^7	-6.272×10^7
butyric	Bu-frag	C4:0	3.862×10^7	2.988×10^7
caproic	Co-frag	C6:0	4.307×10^7	3.347×10^7
caprylic	Cy-frag	C8:0	5.015×10^7	3.808×10^7
capric	C-frag	C10:0	5.292×10^7	4.104×10^7
lauric	L-frag	C12:0	5.707×10^7	4.433×10^7
myristic	M-frag	C14:0	6.006×10^7	4.715×10^7
palmitic	P-frag	C16:0	6.550×10^7	5.077×10^7
palmitoleic	Po-frag	C16:1	6.550×10^7	5.077×10^7
stearic	S-frag	C18:0	6.800×10^7	5.284×10^7
oleic	O-frag	C18:1	6.800×10^7	5.284×10^7
linoleic	Li-frag	C18:2	6.800×10^7	5.284×10^7
linolenic	Ln-frag	C18:3	6.800×10^7	5.284×10^7
arachidic	A-frag	C20:0	7.327×10^7	5.707×10^7
behenic	B-frag	C22:0	7.745×10^7	6.038×10^7
erucic	E-frag	C22:1	7.745×10^7	6.038×10^7

where $C_{p,A}^l$ represents the liquid heat capacity contribution of fragment A in the component (J/(kmol K)), and $N_{frag,A}$ is the number of fragment A in the component.

The heat capacity contribution of fragment A is calculated using the following linear relationship for temperature dependency:

$$C_{p,A}^l = A_{1,A} + A_{2,A}T \tag{5}$$

where $A_{1,A}$ and $A_{2,A}$ are temperature dependency correlation parameters for fragment A and T is the temperature (in Kelvin).

Parameters $A_{1,A}$ and $A_{2,A}$ for the glycerol fragment and the saturated fatty acid fragments with carbon number ranging from 4 to 18 are regressed against literature heat capacity data for temperatures ranging from 298.15 K to 453.15 K.[7,15] The relationships between $A_{1,A}$, $A_{2,A}$, and the carbon number of each fatty acid fragment are shown as the fitting curves eqs (c) and (d) in Table 5. The parameters for the saturated fragments with

Table 7. Calculated Liquid Heat Capacity Fragment Parameters $A_{1,A}$ and $A_{2,A}$

fragment	symbol	carbon	$A_{1,A}$ (J/(kmol K))	$A_{2,A}$ (J/(kmol K²))
glycerol	Gly-frag		6.1355×10^4	148.23
butyric	Bu-frag	C4:0	8.0920×10^4	239.39
caproic	Co-frag	C6:0	1.1557×10^5	308.41
caprylic	Cy-frag	C8:0	1.6402×10^5	304.95
capric	C-frag	C10:0	2.1575×10^5	357.35
lauric	L-frag	C12:0	2.5335×10^5	422.23
myristic	M-frag	C14:0	3.0377×10^5	490.30
palmitic	P-frag	C16:0	3.3036×10^5	616.35
palmitoleic	Po-frag	C16:1	3.3036×10^5	616.35
stearic	S-frag	C18:0	3.6693×10^5	685.76
oleic	O-frag	C18:1	3.9760×10^5	540.89
linoleic	Li-frag	C18:2	3.9760×10^5	540.89
linolenic	Ln-frag	C18:3	3.9760×10^5	540.89
arachidic	A-frag	C20:0	4.1809×10^5	711.23
behenic	B-frag	C22:0	4.6015×10^5	774.15
erucic	E-frag	C22:1	4.6015×10^5	774.15

Table 8. Correlation for Enthalpy of Formation and Double Bond Count in C18 Acid Chains of Simple Triglycerides

pure component properties	trend line equation	R^2
liquid enthalpy of formation	$y = 316.67x - 2466.4$	0.984
solid enthalpy of formation	$y = 324.19x - 2613.2$	1.0

[a] Note: In the equations, y represents the property in column 1 and x represents the double-bond count in C18 acid chains of simple triglycerides. R^2 is the R-square value of the trend line equations.

long chains, such as C20 and C22, can be extrapolated from the linear equations.

The way to account for the unsaturated fatty acid fragments is slightly different from the calculation of vapor pressure, because the heat capacity data of the unsaturated triglyceride triolein [C18:1] are available. We first identify the parameters $A_{1,A}$ and $A_{2,A}$ for the oleic fragment [C18:1], and we treat heat capacities of polyunsaturated triglycerides trilinolein [C18:2] and trilinolenin [C18:3] as identical to those of monounsaturated triolein [C18:1]. Table 7 summarizes the calculated parameters $A_{1,A}$ and $A_{2,A}$ for the glycerol fragment and the fatty acid fragments with carbon numbers ranging from 4 to 22.

Enthalpy of Formation. Enthalpies of formation for various simple triglycerides are first obtained from data for enthalpy of combustion[16−18] and enthalpy of fusion.[12,19,20] The relationships between enthalpy of formation for simple saturated and monounsaturated triglycerides and carbon numbers of the constituent fatty acids are presented as eqs (e)−(h) in Table 5. In addition, Table 8 gives the correlations for the enthalpy of formation and the double-bond count in C18 acid chains of simple triglycerides, including triolein [C18:1], trilinolein [C18:2], and trilinolenin [C18:3].

We further estimate enthalpies of formation for mixed triglycerides as the averages of the simple triglycerides that compose the three fatty acid fragments.

$$\Delta H_{f,\text{mix}}^{\circ} = \sum_{\text{Acid frag}} \frac{N_{\text{Acid frag,A}}}{3} \Delta H_{f,A}^{\circ} \qquad (6)$$

where $\Delta H_{f,\text{mix}}^{\circ}$ is the standard enthalpy of formation of the mixed triglyceride (expressed in units of kJ/mol), $\Delta H_{f,A}^{\circ}$ the standard enthalpy of formation of the simple triglyceride with fatty acid fragment A (also expressed in units of kJ/mol), and $N_{\text{Acid frag,A}}$ the number of the fatty acid A fragments in the mixed triglyceride.

Liquid Molar Volume. The liquid molar volumes of triglycerides are calculated from the fragment composition and the fragment parameters:

$$V^l = \sum_A N_{\text{frag,A}} V_A^l(T) \qquad (7)$$

where V_A^l is the liquid molar volume contribution of fragment (expressed in units of m³/kmol) and $N_{\text{frag,A}}$ is the number of fragment A in the component.

Here, the Van Krevelen equation[21] provides the temperature dependency for the liquid molar volume of fragment A:

$$V_A^l = \frac{1 + B_{2,A}T}{B_{1,A}} \qquad (8)$$

where $B_{1,A}$ and $B_{2,A}$ are the temperature dependency correlation parameters of fragment A, and T is the temperature (in Kelvin).

The parameters $B_{1,A}$ and $B_{2,A}$ for the glycerol fragment and the saturated fatty acid fragments with carbon numbers ranging from 4 to 18 are regressed against available literature experimental density data over a temperature range from 253.15 K to 516.15 K.[22−24] Equations (i) and (j) in Table 5 show the correlations of $B_{1,A}$ and $B_{2,A}$ with carbon numbers of each fatty acid fragments. The parameters of the saturated fragments with long chains, such as C20 and C22, can be extrapolated from the trend line equations.

The parameters $B_{1,A}$ and $B_{2,A}$ of the oleic fragment [C18:1], the linoleic fragment [C18:2], and the linolenic fragment [C18:3] are also regressed against available literature experimental density data.[2,23] Values of $B_{1,A}$ and $B_{2,A}$ for these unsaturated fatty acid fragments with carbon number 18 are listed in Table 9.

Table 9 also summarizes the calculated parameters $B_{1,A}$ and $B_{2,A}$ for the glycerol fragment and the fatty acid fragments with carbon numbers ranging from 4 to 22.

Liquid Viscosity. The liquid viscosities of triglycerides are calculated from the fragment composition and fragment-specific parameters for viscosity:

$$\ln \eta^l = \sum_A N_{\text{frag,A}} \ln \eta_A^l(T) \qquad (9)$$

where $\ln \eta_A^l$ represents the liquid viscosity contribution of fragment A (expressed in units of Pa s) and $N_{\text{frag,A}}$ is the number of fragment A in the component.

The following expression[25] is used to represent the liquid viscosity of fragment A, as a function of temperature:

$$\ln \eta_A^l = C_{1,A} + \frac{C_{2,A}}{T} + C_{3,A} \ln T \qquad (10)$$

where $C_{1,A}$, $C_{2,A}$, and $C_{3,A}$ represent temperature dependency correlation parameters for viscosity and T is the temperature (in Kelvin).

The parameters $C_{1,A}$, $C_{2,A}$, and $C_{3,A}$ for the glycerol fragment and the saturated fatty acid fragments with carbon numbers ranging from 4 to 18 are regressed against available literature experimental viscosity data with a temperature range of 298.15 to 516.15 K.[26−28] Equations (k), (l), and (m) in Table 5 show the correlations of $C_{1,A}$, $C_{2,A}$, and $C_{3,A}$ parameters with carbon numbers of the fatty acid fragments. The parameters for the saturated fragments with long chains, such as C20 and C22, can be extrapolated from the linear equations in Table 5.

Available literature data are also used to identify the effect of double-bond count on the viscosity parameters for the fatty acid fragments. For example, the viscosity parameters of the oleic fragment [C18:1], the linoleic fragment [C18:2], and the linolenic fragment [C18:3] are regressed against the literature experimental

Table 9. Calculated Liquid Molar Volume Fragment Parameters $B_{1,A}$ and $B_{2,A}$

| fragment	symbol	carbon	$B_{1,A}$ (kmol/m^3)	$B_{2,A}$ (K^{-1})
glycerol	Gly-frag		20.048	7.6923×10^{-4}
butyric	Bu-frag	C4:0	18.650	14.503×10^{-4}
caproic	Co-frag	C6:0	12.476	12.385×10^{-4}
caprylic	Cy-frag	C8:0	9.3964	12.232×10^{-4}
capric	C-frag	C10:0	7.6999	12.345×10^{-4}
lauric	L-frag	C12:0	6.5791	12.687×10^{-4}
myristic	M-frag	C14:0	5.7580	13.154×10^{-4}
palmitic	P-frag	C16:0	5.0524	13.008×10^{-4}
palmitoleic	Po-frag	C16:1	5.0524	13.008×10^{-4}
stearic	S-frag	C18:0	4.6326	14.091×10^{-4}
oleic	O-frag	C18:1	4.2924	9.8650×10^{-4}
linoleic	Li-frag	C18:2	4.1679	7.4102×10^{-4}
linolenic	Ln-frag	C18:3	4.3225	8.1078×10^{-4}
arachidic	A-frag	C20:0	4.1168	15.393×10^{-4}
behenic	B-frag	C22:0	3.7693	16.875×10^{-4}
erucic	E-frag	C22:1	3.7693	16.875×10^{-4}

Table 10. Calculated Liquid Viscosity Fragment Parameters $C_{1,A}$, $C_{2,A}$ and $C_{3,A}$

fragment	symbol	carbon	$C_{1,A}$ (Pa s)	$C_{2,A}$ (T in K)	$C_{3,A}$ (T in K)
glycerol	Gly-frag		96.530	-3009.6	-57.439
butyric	Bu-frag	C4:0	-51.003	2546.1	21.264
caproic	Co-frag	C6:0	-51.864	2627.6	21.387
caprylic	Cy-frag	C8:0	-55.104	2867.5	21.843
capric	C-frag	C10:0	-54.786	2919.1	21.784
lauric	L-frag	C12:0	-56.622	3060.8	22.045
myristic	M-frag	C14:0	-59.334	3259.8	22.425
palmitic	P-frag	C16:0	-60.312	3339.1	22.567
palmitoleic	Po-frag	C16:1	-60.312	3339.1	22.567
stearic	S-frag	C18:0	-67.306	3813.5	23.543
oleic	O-frag	C18:1	-53.789	2911.7	21.653
linoleic	Li-frag	C18:2	-39.270	2216.4	19.488
linolenic	Ln-frag	C18:3	-28.757	1491.5	18.027
arachidic	A-frag	C20:0	-66.197	3790.7	23.385
behenic	B-frag	C22:0	-68.231	3954.4	23.669
erucic	E-frag	C22:1	-68.231	3954.4	23.669

data.[11,29−31] Table 10 shows the results of viscosity parameters for the double-bond count of the C18 acid fragments.

Table 10 also summarizes the calculated parameters $C_{1,A}$, $C_{2,A}$, and $C_{3,A}$ for the glycerol fragment and the fatty acid fragments with carbon numbers ranging from 4 to 22.

Estimating Triglyceride Pure-Component Properties. Figures 5−8 respectively show the predicted results of vapor pressure, heat capacity, liquid density, and liquid viscosity for five prevalent simple saturated triglycerides. Heavy-black lines show the predictions with the fragment-based approach. Light-
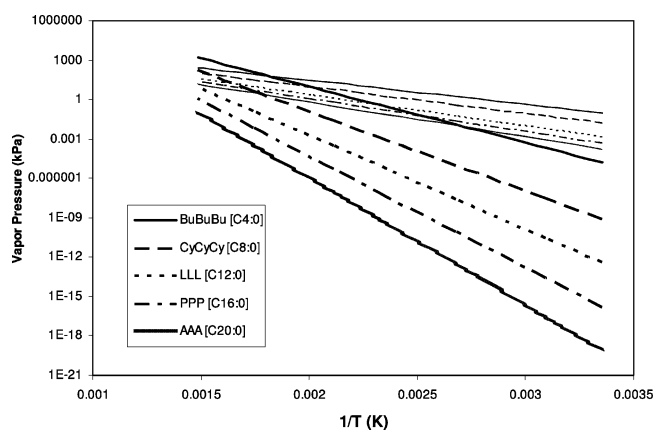
Figure 5. Comparison of predicted vapor pressure of simple saturated triglycerides; heavy-black lines are predictions with the fragment method, light-black lines are predicted with the group contribution method, and lines with the same legend corresponding to the same triglycerides.
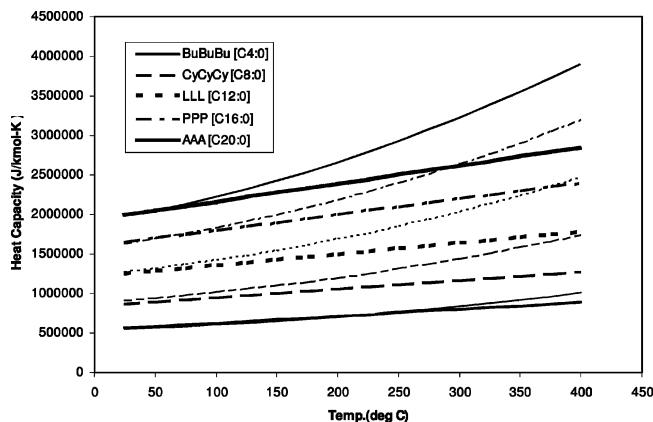
Figure 6. Comparison of liquid heat capacity of simple saturated triglycerides; heavy-black lines are predictions with the fragment method, light-black lines are predicted with the group contribution method, and lines with the same legend correspond to the same triglycerides.
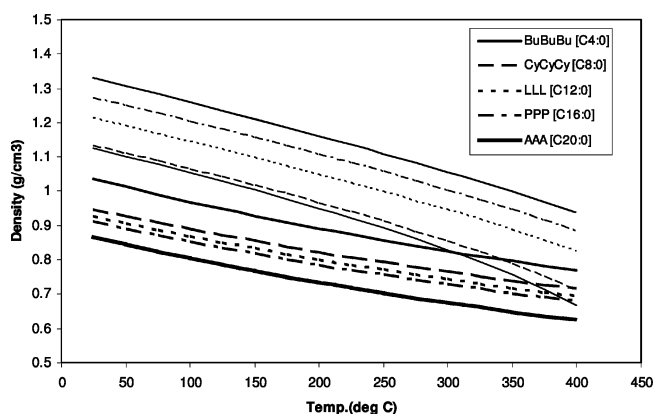
Figure 7. Comparison of liquid density of simple saturated triglycerides; heavy-black lines are predictions with the fragment method, light-black lines are predicted with the group contribution method, and lines with the same legend correspond to the same triglycerides.
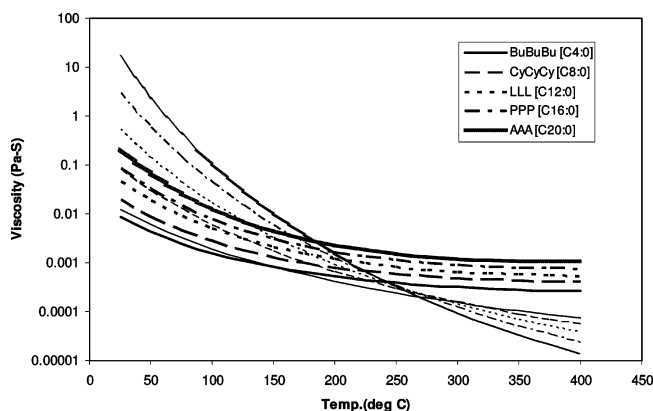
Figure 8. Comparison of liquid viscosity of simple saturated triglycerides; heavy-black lines are predictions with the fragment method, light-black lines are predicted with the group contribution method, and lines with the same legend correspond to the same triglycerides.

black lines are the predictions with the functional group methods available in Aspen Plus. The Li−Ma method,[32] the Ruzicka method,[33,34] the Le Bas method,[4] and the Orrick−Erbar method[4] are the functional group contribution methods used to generate predictions for vapor pressure, heat capacity, liquid density, and liquid viscosity, respectively.

As shown in Figures 5−8, the results predicted by the traditional functional group methods are very different from

Table 11. Triglyceride Composition of Soybean Oil[35]

fatty acid chain	triglyceride	mole fraction soybean oil
C16:0	PPP	0.0379
C18:0	SSS	0.1114
C18:1	OOO	0.2346
C18:2	LiLiLi	0.5439
C18:3	LnLnLn	0.0692

those predicted by our fragment-based approach. Given that the fragment-specific parameters were obtained from fitting against available experimental data for simple triglycerides, the prediction results from the fragment-based approach for simple triglycerides, in fact, represent the available experimental data and the prediction results from functional group methods are far from the data. With the increase in carbon number of simple saturated triglycerides, the trends as predicted by the two different methodologies are similar but the absolute values are very different. Vapor pressures predicted by the Li−Ma functional group approach seem too high by several orders of magnitude. Heat capacities predicted by the Ruzicka functional group method seem to be close to the results from the fragment-based approach. Densities predicted by the Le Bas group contribution method are ~30% too high. Viscosities predicted by the Orrick−Erbar method are orders of magnitude too high at temperatures of <423.15 K and too low at temperatures of >473.15 K.

Estimating Triglyceride Mixture Properties. Vapor Pressure of Soybean Oil. To estimate the properties of oils and fats, the knowledge of the triglyceride composition or fatty acid composition is required. Table 11 presents the triglyceride composition of soybean oil.[35]

To estimate the vapor pressure of soybean oil, which is a triglyceride mixture, we estimate the vapor pressure for each triglyceride in the oil and we apply a mole fraction average mixing rule to calculate the vapor pressure of the oil. As shown in eq 11, this mixing rule is equivalent to the ideal solution assumption, which is reasonable, given that the triglyceride components are similar in molecular structure and size.

$$P_{\text{oil}} = \sum_i x_i P_i \qquad (11)$$

where P_{oil} is the vapor pressure of the oil (expressed in units of Pa), x_i the mole fraction of triglyceride i, and P_i the vapor pressure of triglyceride i (in units of Pa).
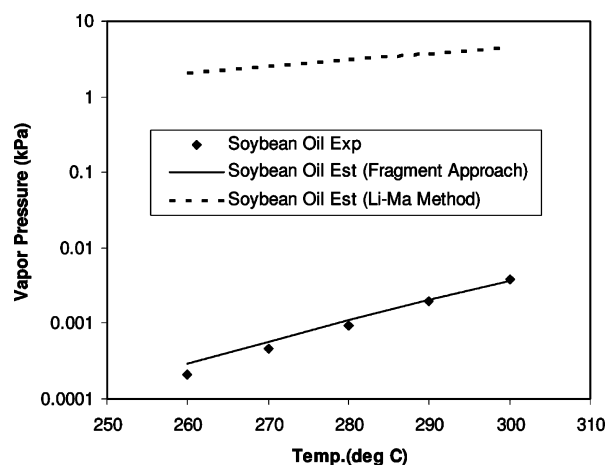
Figure 9 shows the predicted vapor pressure of soybean oil as a function of temperature. Also shown are the predicted results from the Li−Ma group contribution method. The average relative deviation between the vapor pressures of soybean oil predicted with the fragment-based approach and the experimental data[14] is 14%. The Li−Ma group contribution method overpredicts the vapor pressure by 4 orders of magnitude.

Enthalpy of Vaporization of Soybean Oil. Heats of vaporization for triglyceride mixtures can be estimated from heats of vaporization for the triglycerides in the mixture and the mole fraction average mixing rule:

$$\Delta H_{\theta,\text{oil}}^{\text{vap}} = \sum_i x_i \Delta H_{\theta,i}^{\text{vap}} \qquad (12)$$

where $\Delta H_{\theta,\text{oil}}^{\text{vap}}$ is the heat of vaporization of the oil (in units of J/kmol), x_i the mole fraction of triglyceride i, and $\Delta H_{\theta,i}^{\text{vap}}$ the heat of vaporization of triglyceride i (in units of J/kmol).

Table 12 shows the heat of vaporization for "refined" soybean oil.[14] We estimate the heat of vaporization based

Figure 9. Predicted vapor pressure of soybean oil, using experimental data taken from Perry et al.[14]

Table 12. Heat of Vaporization of Soybean Oil

	Heat of Vaporization (298.15 K) (J/kmol)	
oil	estimated	data[14]
soybean oil	1.610×10^8	1.847×10^8

Table 13. Triglyceride Composition of RBDPO and Cocoa Butter[a]

		Mass Fraction	
fatty acid chain	triglyceride	cocoa butter	palm oil (RBDPO)
C14:0	MMM	0	0.0011
C16:0	PPP	0.2594	0.4395
C18:0	SSS	0.3825	0.0265
C18:1	OOO	0.3308	0.4386
C18:2	LiLiLi	0.0231	0.0944
C20:0	AAA	0.0042	0

[a] Data taken from ref 7.

on eq 12, and we assume the triglyceride composition in Table 11.[35] The estimated heat of vaporization with the fragment-based approach is 87% of the value reported for "refined" soybean oil. Given that we do not know the specific triglyceride composition for "refined" soybean oil, we present the results for informational purposes only.

Liquid Heat Capacity of RBDPO and Cocoa Butter. Triglyceride compositions (shown in Table 13) and liquid heat capacities of refined, bleached, deodorized palm oil (RBDPO) and cocoa butter are available in the literature.[7] We predict the heat capacities of the oils with eq 13:

$$C_{p,\text{oil}}^l = \sum_i w_i C_{p,i}^l \qquad (13)$$

where $C_{p,\text{oil}}^l$ is the liquid heat capacity of the oil (expressed in units of J/(g K)), w_i the mass fraction of triglyceride i, and $C_{p,i}^l$ the liquid heat capacity of triglyceride i (in units of J/(g K)).

Figure 10 shows the predicted heat capacities of RBDPO and cocoa butter, as a function of temperature, as well as values determined using the fragment-based approach and the Ruzicka group contribution method, respectively. The predictions of both approaches are in reasonable agreement with the experimental data.[7] The average relative deviations of the fragment-based approach are 0.8% and 2.4% for RBDPO and cocoa butter, respectively. The average relative deviations of the Ruzicka method are 1.7% and 1.4% for RBDPO and cocoa butter, respectively.

Liquid Densities of Three Vegetable Oils. Shown in Table 14 are the triglyceride compositions of three vegetable oils,
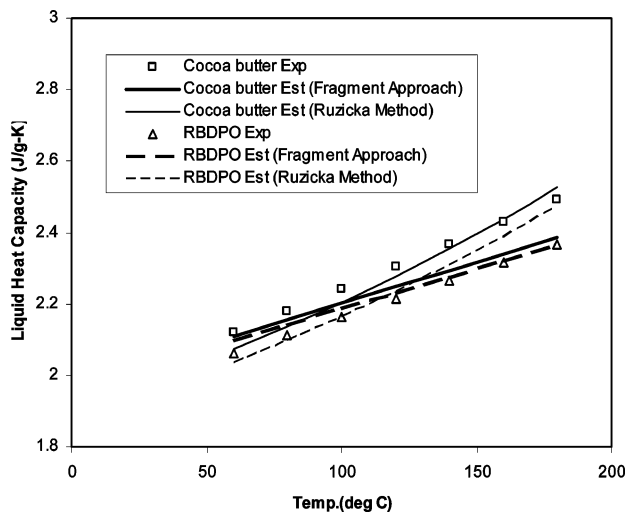
Figure 10. Predicted liquid heat capacity of oils, using experimental data from Morad et al.[7]

Table 14. Triglyceride Composition of Oils[a]

triglyceride	Mass Fraction		
	Brazil nut	Buriti	grape seed
OOO	0.1379	0.4573	0.0373
LiLiLi	0.0386	0	0.3298
POS	0.0408	0.0094	0
SOS	0.0139	0	0
POO	0.1185	0.3521	0.0177
SOO	0.0615	0.0258	0.0064
MSO	0.0341	0.0677	0
PLiP	0.0334	0.0070	0.0095
PLiO	0.1508	0.0204	0.0650
PLiLi	0.0719	0.0118	0.1114
OOLi	0.1748	0.0253	0.1336
OLiLi	0.1238	0.0233	0.2894

[a] Data taken from ref 36.
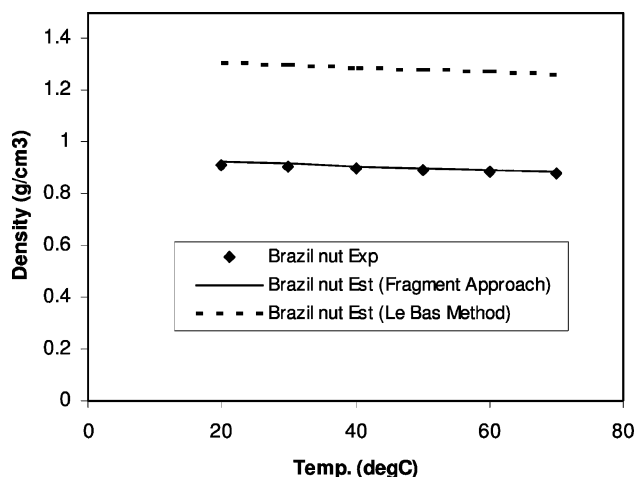
Figure 11. Predicted density of Brazil nut oil, using experimental data from Ceriani et al.[36]

namely, Brazil nut, Buriti, and grape seed.[36] We use the mass fraction averaging rule to estimate densities of these three oils:

$$\frac{1}{\rho_{oil}} = \sum_i w_i \frac{1}{\rho_i} \tag{14}$$

where ρ_{oil} is the liquid density of the oil (expressed in units of g/cm³), w_i the mass fraction of triglyceride i, and ρ_i the liquid density of triglyceride i (in units of g/cm³).
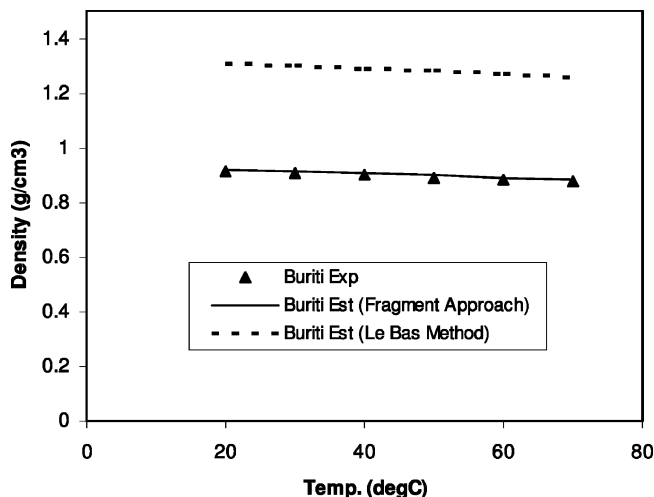

Figure 12. Predicted density of Buriti oil, using experimental data from Ceriani et al.[36]
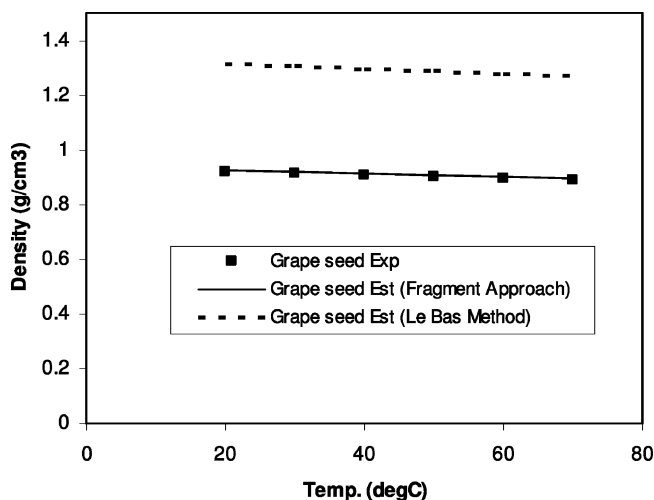

Figure 13. Predicted density of grape seed oil, using experimental data from Ceriani et al.[36]

Figures 11−13 respectively show the estimated densities of Brazil nut oil, Buriti oil, and grape seed oil, each as a function of temperature. Also shown are the predicted results from the Le Bas group contribution method. The predicted densities with the fragment-based approach are in excellent agreement with the experimental data.[36] The average relative deviation for the fragment-based approach is <0.8%, whereas the average relative deviation is 43% for the Le Bas method.

Liquid Viscosities of Three Vegetable Oils. Experimental data for the viscosities of three vegetable oils (Brazil nut, Buriti, and grape seed) are available.[36] We estimate their viscosities based on the weight fraction average mixing rule, eq 15, and the triglyceride composition shown in Table 14.

$$\ln \eta_{oil} = \sum_i w_i \ln \eta_i \tag{15}$$

where η_{oil} is the liquid viscosity of the oil (expressed in units of Pa s), w_i the mass fraction of triglyceride i, and η_i the liquid viscosity of triglyceride i (given in units of Pa s).

Figures 14−16 respectively show the viscosities of Brazil nut oil, Buriti oil, and grape seed oil, each as a function of temperature. The predicted results from the Orrick−Erbar group contribution method are also plotted in the figures as dashed
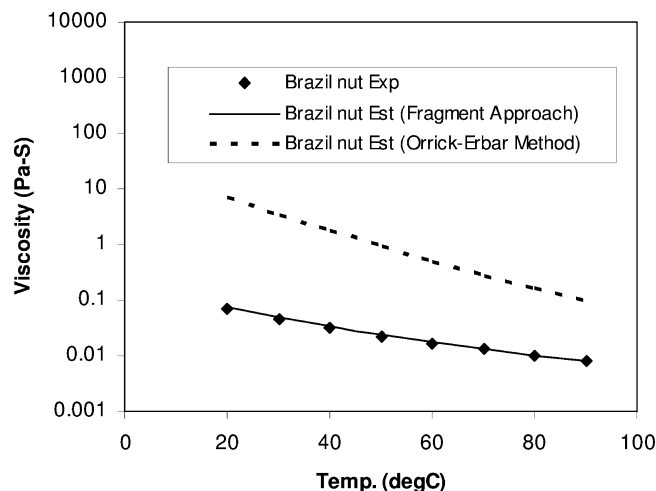
Figure 14. Predicted liquid viscosity of Brazil nut oil, using experimental data from Ceriani et al.[36]
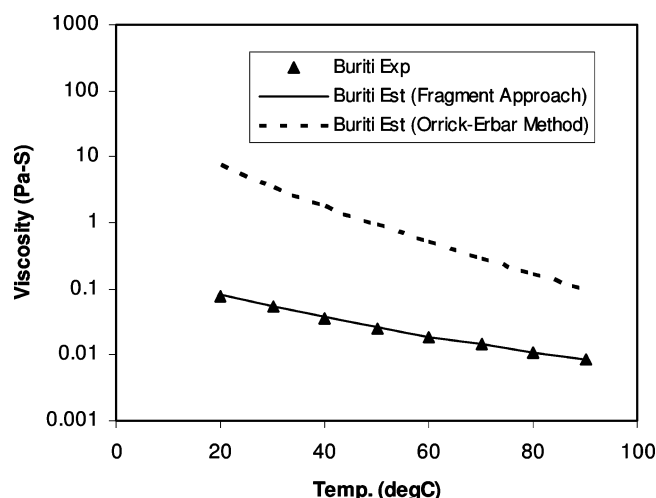

Figure 15. Predicted liquid viscosity of Buriti oil, using experimental data from Ceriani et al.[36]
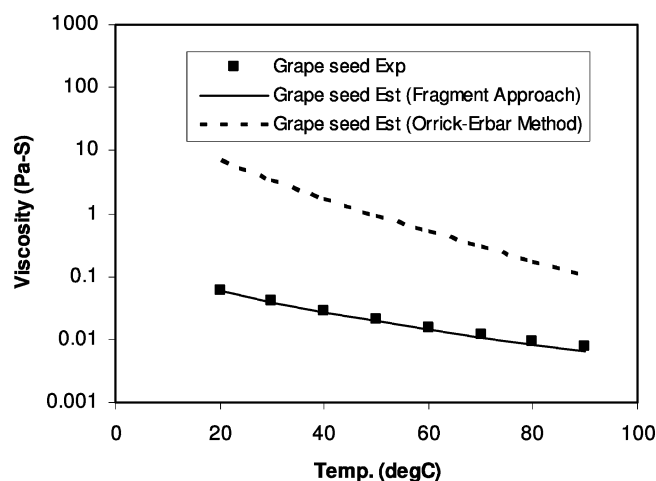

Figure 16. Predicted liquid viscosity of grape seed oil, using experimental data from Ceriani et al.[36]

lines. The predicted liquid viscosities with the fragment-based approach for the three oils are consistent with the experimental data.[36] The average relative deviations for Brazil nut oil, Buriti oil, and grape seed oil are 3.6%, 2.8%, and 8.8%, respectively.

The Orrick−Erbar group contribution method overpredicts the viscosities by 2 orders of magnitude.

Conclusions

This fragment-based methodology enables systematic correlation and accurate estimation of thermophysical properties of triglycerides, fats, and oils. Key features of this method include the constituent fragment-based modeling approach, identification of fragment-specific parameters from limited available literature data, correlation and extrapolation of fragment-specific parameters (each as a function of the fatty acid fragment carbon number), and estimation of double-bond effect. Used with proper mixing rules, the methodology yields superior predictions over those estimated by commonly practiced functional group contribution methods.

The methodology led to the first-ever complete description for thermophysical properties of triglycerides, fats, and oils. It enables development of a triglyceride thermophysical property databank, which contains, among other properties, vapor pressure, enthalpy of vaporization, liquid heat capacity, enthalpy of formation, liquid molar volume, and liquid viscosity. This triglyceride databank, together with the existing Aspen Plus databank and Aspen NIST databank for thermophysical properties of fatty acids and their corresponding methyl esters, provides efficient and reliable thermophysical property calculation capability essential for process modeling, simulation, design, and optimization of biodiesel production processes.

Literature Cited

(1) http://en.wikipedia.org/wiki/Triglyceride, accessed on July 14, 2009.

(2) Sum, A. K.; Biddy, M. J.; de Pablo, J. J. Predictive Molecular Model for the Thermodynamics and Transport Properties of Triacylglycerols. *J. Phys. Chem. B* **2003**, *107*, 14443–14454.

(3) Bockisch, M., *Fats and Oils Handbook*; AOCS Press: Champaign, IL, 1998.

(4) Poling, B. E., Prausnitz, J. M., O'Connell, J. P. *The Properties of Gases and Liquids*, 5th Edition; McGraw−Hill: New York, 2000; pp 4.33 and 9.59−9.61.

(5) Ceriani, R.; Meirelles, A. J. A. Predicting Vapor-liquid Equilibria of Fatty Systems. *Fluid Phase Equilib.* **2004**, *215*, 227–236.

(6) Antoniosi Filho, N. R.; Mendes, O. L.; Lancas, F. M. Computer Prediction of Triacylglycerol Composition of Vegetable Oils by HRGC. *Chromatographia* **1995**, *40*, 557–562.

(7) Morad, N. A.; Kamal, A. A. M.; Panau, F.; Yew, T. W. Liquid Specific Heat Capacity Estimation for Fatty Acids, Triacylglycerols, and Vegetable Oils Based on Their Fatty Acid Composition. *J. Am. Oil Chem. Soc.* **2000**, *77*, 1001–1005.

(8) O'Brien, R. D. *Fats and Oils Formulating and Processing for Applications*, 2nd Edition; CRC Press: Boca Raton, FL, 2003; pp 6−8.

(9) http://www.scientificpsychic.com/fitness/fattyacids1.html, accessed on July 14, 2009.

(10) Hui, Y. H. *Handbook of Food Science, Technology, and Engineering*, Vol. 4; Marcel Dekker: New York, 2005; pp 155.2−155.3.

(11) Ceriani, R.; Goncalves, C. B.; Rabelo, J.; Caruso, M.; Cunha, A. C. C.; Cavaleri, F. W.; Batista, E. A. C.; Meirelles, A. J. A. Group Contribution Model for Predicting Viscosity of Fatty Compounds. *J. Chem. Eng. Data* **2007**, *52*, 965–972.

(12) Zéberg-Mikkelsen, C. K.; Stenby, E. H. Predicting the Melting Points and the Enthalpies of Fusion of Saturated Triglycerides by a Group Contribution Method. *Fluid Phase Equilib.* **1999**, *162*, 7–17.

(13) Clarke, E. C. W.; Glew, D. N. Evaluation of Thermodynamic Functions from Equilibrium Constants. *Trans. Faraday Soc.* **1966**, *62*, 539–547.

(14) Perry, E. S.; Weber, W. H.; Daubert, B. F. Vapor Pressure of Phlegmatic Liquids I. Simple and Mixed Triglycerides. *J. Am. Chem. Soc.* **1949**, *71*, 3720–3726.

(15) Phillips, J. C.; Mattamal, M. M. Correlation of Liquid Heat Capacities for Carboxylic Esters. *J. Chem. Eng. Data* **1976**, *21*, 228–232.

(16) Domalski, E. S. Selected Values of Heats of Combustion and Heats of Formation of Organic Compounds Containing the Elements C, H, N, O, P, and S. *J. Phys. Chem. Ref. Data* **1972**, *1*, 222–277.

(17) Freedman, B.; Bagby, M. O. Heats of Combustion of Fatty Esters and Triglycerides. *J. Am. Oil Chem. Soc.* **1989**, *66*, 1601–1605.

(18) Krisnangkura, K. Estimation of Heat of Combustion of Triglycerides and Fatty Acid Methyl Esters. *J. Am. Oil Chem. Soc.* **1991**, *68*, 56–58.

(19) Hampson, J. W.; Rothbart, H. L. Heats of Fusion for Some Triglycerides by Differential Scanning Calorimetry. *J. Am. Oil Chem. Soc.* **1969**, *46*, 143–144.

(20) Hagemann, J. W.; Tallent, W. H. Differential Scanning Calorimetry of Single Acid Triglycerides: Effect of Chain Length and Unsaturation. *J. Am. Oil Chem. Soc.* **1972**, *49*, 118–123.

(21) Van Krevelen, D. W. *Properties of Polymers*, 3rd Edition; Elsevier: Amsterdam, 1990.

(22) Nilsson, S.-O.; Wadso, I. Thermodynamic Properties of Some Mono-, Di-, and Tri-Esters. Enthalpies of Solution in Water at 288.15 to 318.15 K and Enthalpies of Vaporization and Heat Capacities at 298.15 K. *J. Chem. Thermodynam.* **1986**, *18*, 673–681.

(23) Jaeger, F. M. Temperature Dependence of the Free Surface Energy of Liquids in Temperature Range from −80 to 1650 degrees Centigrade. *Z. Anorg. Allg. Chem.* **1917**, *101*, 1–214.

(24) Phillips, J. C.; Mattamal, G. J. Effect of Number of Carboxyl Groups on Liquid Density of Esters of Alkylcarboxylic Acids. *J. Chem. Eng. Data* **1978**, *23*, 1–6.

(25) Reid, R. C., Prausnitz, J. M., Poling, B. E. *The Properties of Gases and Liquids*, 4th Edition; McGraw−Hill: New York, 1987; p 439.

(26) Rodriguez, M.; Galan, M.; Munoz, M. J.; Martin, R. Viscosity of Triglycerides + Alcohols from 278 to 313 K. *J. Chem. Eng. Data* **1994**, *39*, 102–105.

(27) Kishore, K.; Shobha, H. K.; Mattamal, G. J. Structural Effects on the Vaporization of High Molecular Weight Esters. *J. Phys. Chem.* **1990**, *94*, 1642–1648.

(28) Niir, B. *Modern Technology of Oils, Fats and Its Derivatives*; National Institute of Industrial Research: New Delhi, 2000; pp 9−11.

(29) Eduljee, G. H.; Boyes, A. P. Viscosity of Some Binary Liquid Mixtures of Oleic Acid and Triolein with Selected Solvents. *J. Chem. Eng. Data* **1980**, *25*, 249–252.

(30) Exarchos, N. C.; Tasioula-Margari, M.; Demetropoulos, I. N. Viscosities and Densities of Dilute Solutions of Glycerol Trioleate + Octane, + *p*-xylene, + Toluene, and + Chloroform. *J. Chem. Eng. Data* **1995**, *40*, 567–571.

(31) Valeri, D.; Meirelles, A. J. A. Viscosities of Fatty Acids, Triglycerides, and Their Binary Mixtures. *J. Am. Oil Chem. Soc.* **1997**, *74*, 1221–1226.

(32) Li, P.; Ma, P.-S.; Yi, S.-Z.; Zhao, Z.-G.; Cong, L.-Z. A New Corresponding-States Group-Contribution Method (CSGC) for Estimating Vapor Pressure of Pure Compounds. *Fluid Phase Equilib.* **1994**, *101*, 101–119.

(33) Ruzicka, V., Jr.; Domalski, E. S. Estimation of the Heat Capacities of Organic Liquids as a Function of Temperature Using Group Additivity. I. Hydrocarbon Compounds. *J. Phys. Chem. Ref. Data* **1993**, *22*, 597–618.

(34) Ruzicka, V., Jr.,; Domalski, E. S. Estimation of the Heat Capacities of Organic Liquids as a Function of Temperature Using Group Additivity. II. Compounds of Carbon, Hydrogen, Halogens, Nitrogen, Oxygen, and Sulfur. *J. Phys. Chem. Ref. Data* **1993**, *22*, 619–657.

(35) Ndiaye, P. M.; Tavares, F. W.; Dalmolin, I.; Dariva, C.; Oliveira, D.; Oliveira, J. V. Vapor Pressure Data of Soybean Oil, Castor Oil, and Their Fatty Acid Ethyl Ester Derivatives. *J. Chem. Eng. Data* **2005**, *50*, 330–333.

(36) Ceriani, R.; Paiva, F. R.; Goncalves, C. B.; Batista, E. A. C.; Meirelles, A. J. A. Densities and Viscosities of Vegetable Oils of Nutritional Value. *J. Chem. Eng. Data* **2008**, *53*, 1846–1853.